

Climate change strongly affects future fire weather danger in Indian forests

Anasuya Barik ¹✉ & Somnath Baidya Roy ¹✉

Changes in temperature, precipitation, wind speed, and relative humidity due to climate change are likely to alter future fire regimes. We quantified the impact of such changes on the fire weather of Indian forests using a fire weather index and high-resolution downscaled climate projections. While conventional wisdom contends that future temperature increases will increase fire weather indices, we find this to be true only in dry forests. In humid forests, the fire weather index will decrease despite the warming due to future increases in precipitation and/or relative humidity. Days with severe fire weather danger will increase by up to 60% in dry forests but will reduce by up to 40% in humid forests. The fire season will be longer by 3–61 days across the country and the pre-monsoon fire season will become more intense over 55% of forests. This study suggests for countries like India with fragmented forests and diverse ecoclimates, standards and mitigation strategies must be developed at regional instead of national level.

¹Indian Institute of Technology Delhi, Hauz Khas, New Delhi, India. ✉email: Anasuya.Barik@cas.iitd.ac.in; drsbr@iitd.ac.in

Climate change is leading to severe fire regimes in the global forests^{1–6}. The intensities and frequencies of fire events are likely to change in the future with changing climate^{6–11}. There is also evidence of the lengthening of fire seasons in the future^{12–14}. IPCC AR6 reports with high confidence that some regions will be subjected to more severe fire weather conditions. It also predicts that the mean fire season length will increase by about 50 days in a 4° warmer climate compared to the 1981–2000 baseline¹⁵.

Almost 21% of India is covered by forests that are home to a wide range of species making Indian forests a biodiversity hotspot¹⁶. The forest types are extremely diverse ranging from arid to alpine. Most forests are heavily fragmented due to high human population density and intense land use practices¹⁷. Forest fires occur throughout the year except for the peak monsoon period¹⁶. According to climate projections, India will experience a warming of 4.4–4.8 °C by the end-century as compared to the 1976–2005 period^{18,19}. Such warming is expected to affect forest fire occurrences and severity in India. However, other factors like future changes in humidity and precipitation are also likely to play pivotal roles in the future fire regime^{20,21}. Furthermore, climate change may affect the timing and intensity of the monsoons. Despite the prevalence of forest fires, their implications on biodiversity, and evidence of rapidly changing climate patterns, there are no comprehensive country-scale studies that attempt to understand and quantify the fire-climate interplay in India. Most regional fire-climate interaction studies are from dry subtropical forests and we cannot draw meaningful inferences from those studies about forest fires in India. Existing global-scale studies simulate fire weather over the entire world, including India, but they do not generally analyze the results over India. Potentially, we could gain some information on the fire danger over India by visually inspecting the global maps, but they would be inadequate for three reasons. First, the typical 0.5–2° spatial resolution of the global studies is too coarse to resolve the fragmented forests of India. Second, the results are widely divergent, from an overall homogenous increase^{2,22,23}, an increase in the northwestern part and a decrease in the rest of India^{9,24}, to a decrease in the mean FWI signal in all regions²⁵, in future fire danger. Such inconsistencies in findings are due to differences in a host of factors including the resolution and quality of climate inputs, the land cover data, and the structure of the dynamic fire modules. The third limitation, as pointed out by Liu et al.⁷ is the lack of forest masks leading to unrealistic results such as high fire danger in the deserts of northwestern India. Our study improves the state of science by simulating the fire weather at high granularity along with a forest mask using a well-calibrated and validated model to advance our understanding of fire-climate interactions in this understudied region.

Forest fires are driven by many factors like weather, vegetation, fuel loading, and local socioeconomic conditions. Among the important factors, climate change has a direct and the largest impact on fire weather. Fire weather is the state of meteorological variables like temperature, relative humidity, precipitation, and wind over a forest ecosystem that affects the fuel loading and controls the start and spread of fires^{10,26–28}. A warmer atmosphere helps the available fuel reach its ignition temperature faster^{12,13}. Relative humidity (RH) impacts the fuel loading by regulating the fuel moisture in surface vegetation^{13,29}. Wind impacts the dryness of the surface fuel and controls the fire spread by controlling the combustion process¹⁰. Precipitation dampens the available surface and subsurface fuel and decreases the probability of fire occurrence³⁰. The probability of fire occurrence becomes zero beyond a certain threshold value of rainfall³¹. Climate change will impact these meteorological variables and thus the future fire weather³². This study uses a high-resolution climate projection

Downscaled CESM (DSCESM)³¹ to fire weather and estimates these impacts over India.

FWI is a metric that systematically integrates the individual and combined effects of the meteorological variables to represent fire danger. The Canadian Forest Fire Danger Rating System–Fire Weather Index (CFFDRS-FWI)^{33–35} is a widely used system for computing FWI. It has been applied in many regional and global-scale applications after appropriate calibration^{36–41}. Here, we used the CFFDRS-FWI driven by meteorological variables from the DSCESM data (“Methods”) to compute FWI over a 3680 × 3680 km study domain centered around India. The domain was discretized with a 10 km grid, which is the same resolution as the DSCESM data. The simulations were run with a daily timestep for 2 time slices which we termed as (1) baseline (2006–2015) and (2) end-century (2091–2100) under the RCP8.5 climate change scenario. We quantitatively estimated the relationship between the simulated FWI for the baseline period and the observed MODIS active fire data⁴² for every grid cell using three non-parametric tests and a fire count per percentile of FWI analysis (“Methods”). The simulated baseline FWI was also used in conjunction with the observed fire count for each grid cell to estimate the threshold FWI values for five fire danger classes based on an ensemble of five different approaches (“Methods”). The FWI for the end-century case was then compared with the baseline case to estimate the changes in the mean annual FWI and identify the major meteorological driver resulting in these changes. We also analyzed the changes in severe fire weather days, the fire weather danger season, and the Seasonal Severity Rating (SSR) in the future due to changing climate.

Results

Forest classification. India has very diverse forest types ranging from arid, to tropical to alpine and different climatic zones^{43,44}. Hence, the impact of climate change on fire regimes is likely to differ for different types of forests. To account for these variations, we classified the study area into five major FWI zones (Fig. 1). This classification was done by combining Köppen’s classification of climatic zones over India⁴³ and a satellite-based land use/land cover map⁴⁴. The five zones are (1) the cold, dry Himalayan mountainous region (HIM) covered by alpine and subtropical pine forests, (2) the warm, humid North-east (NE) with wet evergreen and deciduous forests, (3) the hot, dry Central India (CEN) with mixed deciduous and tropical thorn forests, (4) the hot, dry Deccan (DEC) thorn forest and (5) the warm, humid Western Ghats (WG) with semi-evergreen forests. The CFFDRS-FWI was calibrated, and the future fire projections were analyzed separately for each zone.

Relationship between FWI and observed fire count. The baseline FWI simulated by CFFDRS is strongly correlated with the observed MODIS fire count over forested grid cells. We used three non-parametric tests to statistically test if any non-random relationship existed between fire count and FWI (“Methods”). The Chi-square test of association/independence⁴⁵ shows that the two variables are correlated at $p < 0.05$. The Yule’s correlation⁴⁶ between the two is 0.88 which is significant at $p < 0.05$. Fisher’s exact test⁴⁷ indicates a non-random relationship significant at $p < 0.05$. The Fisher’s odds ratio is 16.74 at a 99% significance level which implies that the odds are 16.74 times higher that fire will occur at low FWI values compared to high FWI. Overall, these tests show that FWI can be considered an appropriate metric to represent fire occurrence.

The maps of the annual mean FWI percentile for the baseline case and the observed MODIS fire count for the same period (Fig. 2-i) show that there is a spatial correspondence between fire

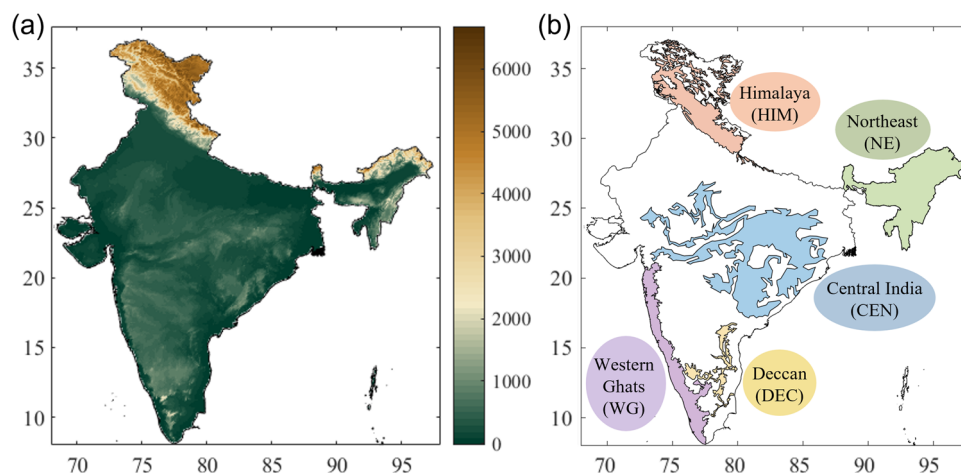


Fig. 1 FWI zones over India. Study area depicting **a** topography and **b** classified FWI Zones over India.

count and FWI. Grid cells with high fire counts have higher (above the 40 percentile) FWI values. For example, NE has a high FWI and extremely high fire count due to high anthropogenic ignition from the prevalence of shifting cultivation practices^{48,49}. Bedia et al.⁵⁰ also reported a high correlation between burned area and FWI averaged over the fire season in this region. Similar signatures of higher FWI and corresponding high fire occurrence can be observed in HIM, southern CEN, northern WG, and DEC.

To further study the association between FWI and fire count, we plotted a scatterplot of fire count vs. the FWI percentile values corresponding to the fire events (Fig. 2-ii). This is slightly different from the spatial map where we averaged over all FWI values irrespective of whether fire has occurred or not. We observe a strong relationship between FWI and fire count with more (less) fire events at high (low) FWI values for all the forest zones (Fig. 2). However, the nature of the relationship varies by forest zones. The best-fit curves with the highest values of coefficient of determination show that the relationship is exponential in the case of the NE zone (Fig. 2b) but cubic in the HIM, CEN, DEC, and WG zones (Fig. 2a, c–e). As discussed later, this difference has implications for developing FWI thresholds for fire severity classes for different forest zones. Overall, both plots suggest that high FWI is an important requirement for fire occurrence and hence confirm earlier findings that FWI is a good metric to estimate fire danger^{36–40}.

We estimated five threshold FWI values to represent five fire danger classes: Low, Medium, High, Very High, and Extreme (“Methods”). The most common approach³³ considers a certain percentage of days as extreme fire days and then uses geometric progression to compute the other thresholds. When we used this default approach using 3% of days as extreme fire days, we observed that the conditional probability (Fig. 3a) in CEN, DEC, and WG regions saturates at 1 from the Medium class of the default approach. Ideally, the probabilities should increase gradually for each class from Low to Extreme for a reliable representation of increasing fire danger. If the maximum probability occurs at Medium threshold itself, the classification becomes less effective in conveying the gradation of fire danger. Hence, we used an ensemble of five other approaches (“Methods”). We observe that the conditional probabilities of the ensemble approach increase gradually for each class and saturate at the Extreme class except for WG where it saturates at the Very High class (Fig. 3a). Also, the threshold computation by default approach considers only the distribution of FWI. The ensemble approach additionally accounts for aspects like fire occurrence probability, the percentage of fires occurring in each class, and

machine learning-based FWI clusters. This makes the resulting thresholds for each danger class more robust.

Figure 3b shows the computed limiting values of the fire danger classes for each zone. One interesting pattern that stands out is that the NE zone has a lesser FWI threshold for all fire danger classes compared to the other zones. For example, Medium fire danger occurs at a FWI value of 2.5 for NE while the corresponding range for the other forests is 3–3.3. Similarly, the FWI thresholds for Extreme fire danger is 3.5 for NE but for other forests, the thresholds are in the 4.3–4.8 range. This difference between NE with the other forest zones is corroborated by Fig. 2-ii which shows that the best-fit curve in this region is different from the others.

This different behavior of NE can be attributed to factors including terrain, biomass density, species composition, and ignition factors. The higher fuel loading in the relatively denser NE forests is one of the major reasons for higher fire activity even in lower FWI⁴⁹. In this zone, most of the open forests practice shifting cultivation. This predominant source of anthropogenic ignition makes this region fire-prone even at low FWI values^{48,49}, especially during the pre-monsoon season^{51,52}. In the other zones, the climates are drier than NE, leading to relatively high FWI. In some parts of CEN and DEC, forests are scattered and are dominated by mixed deciduous and tropical dry thorn forest types. Fire events are usually ground fires scattered around the periphery of core forest zones. Lack of combustible dry fuel due to human interventions and less biomass density lead to comparatively fewer fires in these regions even sometimes with higher FWI conditions⁵³. In HIM, the high-altitude forests are cloaked with snow for a few months in the year. This limits the fire activity at high FWI conditions during those times.

Our analysis shows that it is not appropriate to use the same FWI thresholds over the entire country. The fire danger classes must be defined using different thresholds for different forest zones of India. This clearly demonstrates the value of conducting high-resolution analysis that allows us to capture the spatiotemporal variability of weather patterns and forest types across the country.

Change in annual mean FWI. We analyzed the projected change in annual mean FWI by comparing the end-century average FWI with the baseline (Fig. 4a). The figure shows that fire weather is projected to increase in northern CEN, southern WG, NE, and most of the HIM zone. Western CEN and northern WG show a decrease in mean projected FWI. To understand the reasons

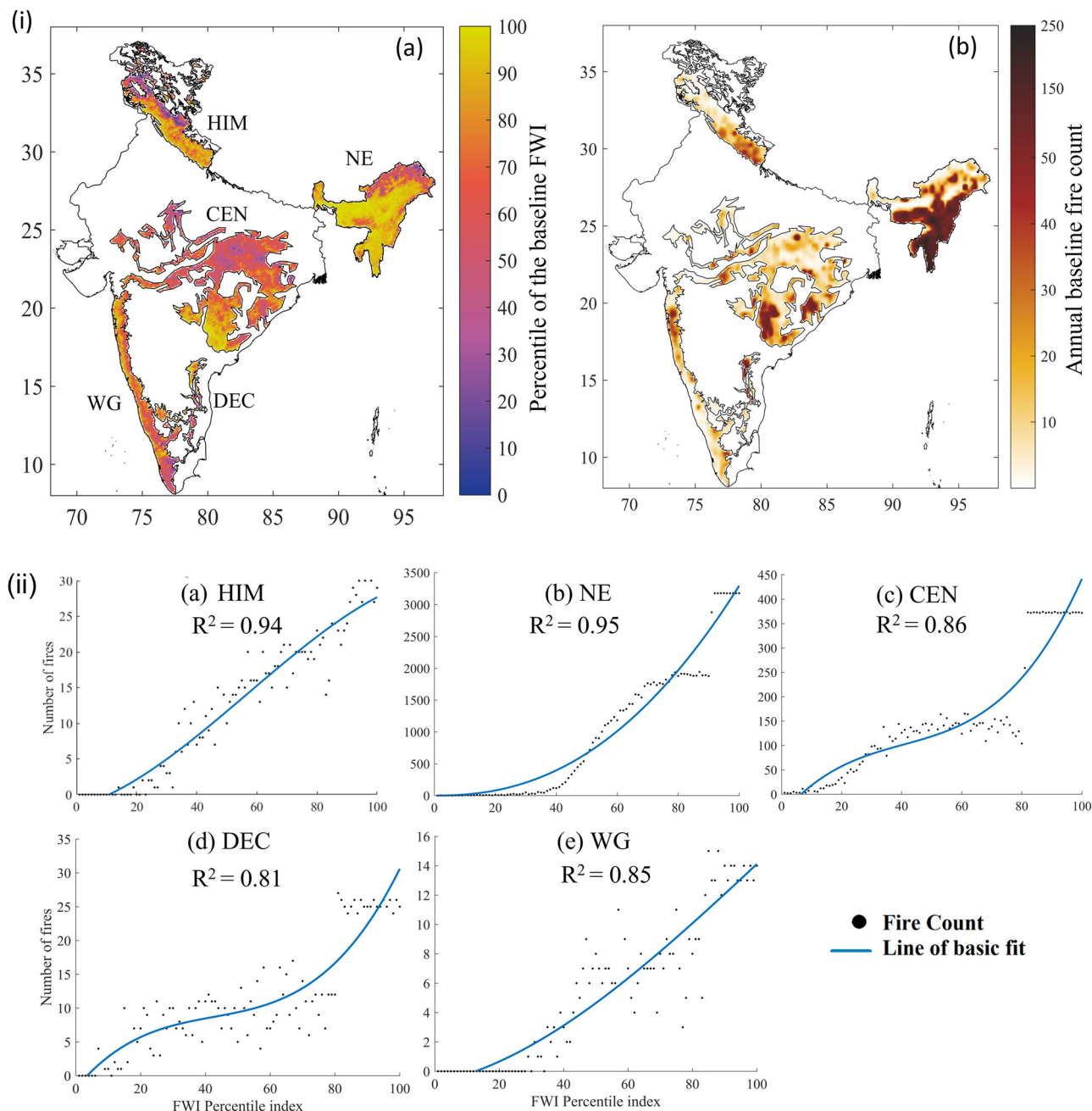


Fig. 2 Relationship between FWI and fire count. Relationship between fire counts and percentiles of FWI. (i) Spatial map of **a** percentiles of annual mean FWI and **b** MODIS observed annual fire count and (ii) scatterplot of fire count for each FWI percentile bin for **a** HIM, **b** NE, **c** CEN, **d** DEC, and **e** WG FWI zones for the baseline period (2006–2015). R^2 represents the coefficient of determination.

behind these changes, we plotted a map showing which variable contributes most to the FWI change for each pixel (“Methods”; Fig. 4-ib). We also compared the dominant contributor information with a modified de Martonne’s aridity index^{54,55} (“Methods”) in each pixel. We observe that in the arid and intermediate regions, temperature is the major contributor to the projected change in FWI (Fig. 4-ic, d). However, in humid regions, precipitation and/or relative humidity play a more important role than temperature (Fig. 4-ie). For example, in the humid NE zone, climatological FWI will decrease majorly due to the increase in annual precipitation. However, the decrease in climatological FWI in the humid region of northern WG is majorly governed by the increase in relative humidity. Temperature is the dominant factor causing the change in future FWI

in the arid and intermediate regions of CEN, southern WG, and DEC.

To analyze the change in the mean annual shift in FWI expected by the end-century, we computed the Kernel Density Estimation (KDE) distribution of mean FWI for different forest zones for both time slices. Figure 4-ii shows that the KDE distribution curves in all zones are multimodal. The distribution curve is skewed most toward higher FWI values in the CEN zone where the hot and arid climate persists for most of the year⁴³. In the NE and HIM regions, the values are skewed mostly toward the left indicating comparatively low overall FWI values. In HIM, this can be attributed to relatively colder temperate temperatures. However, in NE, it is majorly the wetter tropical monsoon climate that causes lower FWI values. Even though NE has a distinct peak

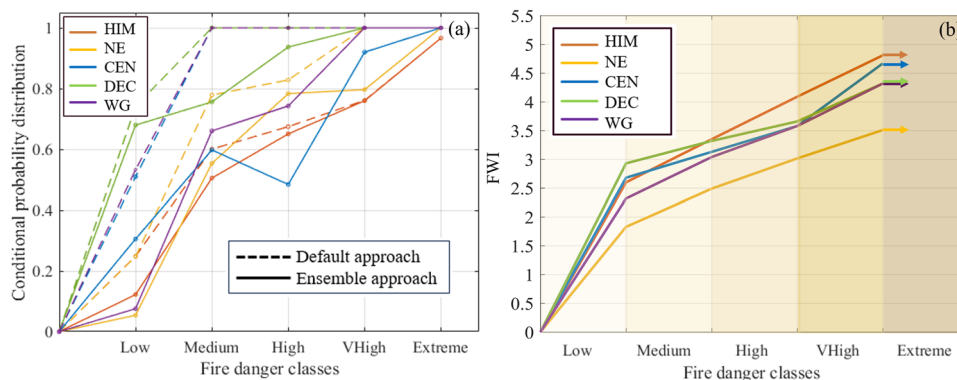


Fig. 3 Fire danger classes using ensemble approach. Thresholds defined for fire danger classes. **a** Conditional probability distribution of fire counts corresponding to the limiting FWI values of fire danger classes for the default and ensemble approach and **b** upper threshold values of FWI defining 5 fire danger classes for different forest zones using the ensemble approach.

in KDE at low FWI values, the frequency and severity of fires in these regions remain high due to terrain, species composition, and ignition factors^{48,56}. This also justifies the requirement for a lower danger threshold in this region. In WG, several peaks in KDE are observed. The peaks in low FWI values can be attributed to the humid climate prevailing in that zone during the southwest monsoon season. The heavy precipitation during this period prevents fire occurrences. Almost no fire activity during the low FWI period maintains the fire danger threshold higher as compared to NE (Fig. 3).

The KDE curves for the end-century shift toward the right from baseline with $p > 0.05$ in all forest zones. This indicates overall higher FWI values in the end-century than the baseline corresponding to a particular value of probability density. To quantify the extent of the shift in FWI by the end-century, we computed the bootstrapped mean values of the kernel distributions at 95% significance. Results show an overall increase of 5–10% in mean FWI by the end-century. The CEN region shows the maximum difference of about 0.54 while the least difference was in the NE zone of about 0.09 FWI. We also observe some parts of the KDE curve in NE and WG (Fig. 4-ia, c) where the end-century curve shifts to the right indicating lower future FWI.

Spatial pattern of severe FWI days. We analyzed the spatial pattern of expected changes in severe fire weather days by end-century. For this, we plotted maps of the number of days per grid cell when FWI values exceeded Medium, High, and Very High thresholds under baseline climate conditions and also how the number of days could change under future conditions (Fig. 5). Results show that there is considerable diversity between, and even within, different forest zones. Currently, large parts of the CEN, NE, and WG forests are under threat of Medium, High, and Very High fire weather for more than 150, 50, and 30 days a year, respectively. The HIM forest experiences the lowest fire weather danger.

Forest types most prevalent in these threatened regions are dry deciduous forests in western CEN, moist deciduous forests in NE and northern WG, and semi-evergreen forests in southern NE⁵². Satellite and ground-based fire observations in India suggest that tropical dry deciduous forests experience the highest fire events closely followed by tropical evergreen forest class^{52,57–59}. High susceptibility of tropical evergreen forests toward fire events has also been observed in Indonesia⁶⁰.

By the end-century, large parts of forested areas are likely to experience an increase in the days with severe fire weather. The moist deciduous forests in the Himalayan foothills (HIM) and the southern part of NE, the dry deciduous forests in eastern CEN

and DEC, and the tropical evergreen forests in the northern part of WG will face increased hazards in all three danger classes. These regions are likely to experience a 20–60% increase in severe FWI days. Regions of maximum concern where extreme fire weather danger days would increase by 30–50 days per year are the *Cachar* semi-evergreen and mixed moist deciduous forests in the states of Tripura and Mizoram, *Chir pine* and *Sal* forests in the Himalayan foothills, the northern moist evergreen forests in the Western Ghats, and the southern mixed deciduous forests in the states of Orissa and Andhra Pradesh. Similar increases in fire disturbance due to climate change have also been observed in Northwestern USA⁶¹, projected in Canada⁶² and various other parts of the globe^{7,24,25,50}.

Some forest areas can experience a decrease in severe fire weather days. It is interesting to note that opposite signals can occur within the same forest zones such as in NE, CEN, and WG. The western part of CEN is likely to show a decrease in the number of High and Very High FWI days by the end-century whereas the eastern part shows an increase. This is different from the signal of climatological change in FWI (Fig. 4-ia). In the northern CEN, though the mean FWI is expected to increase in the future, the number of days having severe days will decrease. This is because the mean FWI increase is driven by the increase in temperature over that region (Fig. 4-ib). However, the DSCESM precipitation projections show that the daily rainfall amounts would increase in 70% of the days in the future. More number of wetter days in an extended monsoon season would result in higher fuel moisture content and hence, fewer days with severe FWI in the future. In another example, the northern part of WG shows an increase in high FWI days but the signal of change is negative in the central and southern parts. This difference also can be attributed to the different variables playing the key role in causing the change. In the southern WG, the mean FWI change signal is majorly governed by DSCESM projected ~2.1 °C increase in mean annual temperature whereas in the southern WG, a 40% increase in the mean relative humidity lowers the future FWI. However, the number of high FWI days signal is governed by the projected increase in precipitation events, which is stronger in the south than in the northern WG. In the central NE region, days exceeding all three thresholds would decrease in the future. This is also due to increased mean annual rainfall, which is the key contributor variable identified in that region (Fig. 4-ib).

Seasonal pattern of fire weather severity. We used the Seasonal Severity Rating (SSR) to study the seasonal pattern of fire weather severity and how it may change due to changing climate. SSR is a numeric index derived from FWI and is a metric representing the

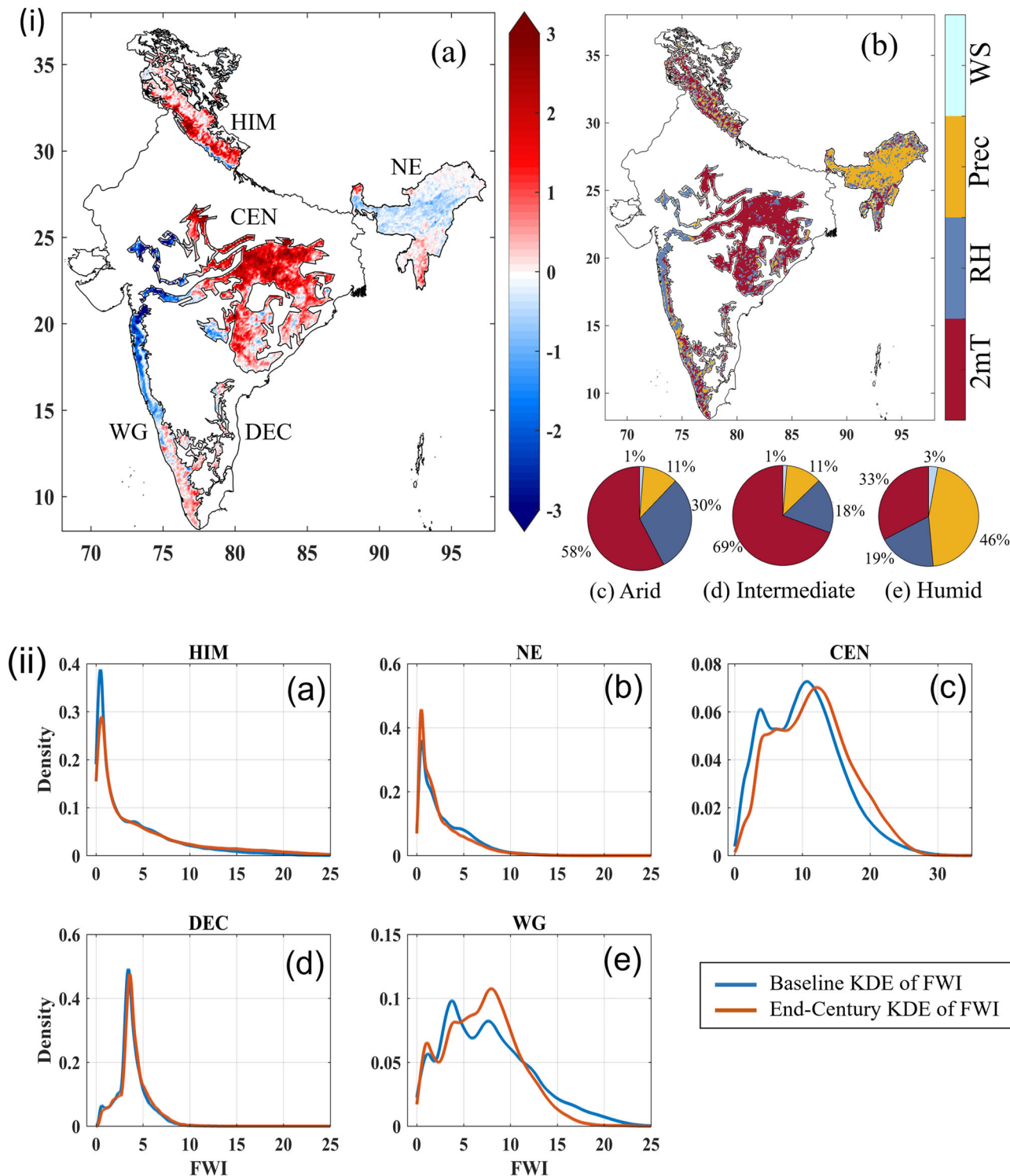


Fig. 4 Change in mean FWI signal between baseline and end-century. Future change in mean FWI signal. **(i) a** Spatial map of the change in mean annual FWI between baseline and end-century, **b** variable contribution resulting in this change, pie charts of dominant contributor in **c** arid, **d** intermediate, and **e** humid regions and **(ii)** Kernel density estimation (KDE) for baseline and future daily FWI for **a** HIM, **b** NE, **c** CEN, **d** DEC, and **e** WG FWI zones.

difficulty in controlling fire events on a seasonal scale (“Methods”). Figure 6-i shows that the most severe fire weather occurs in MAM. Satellite and ground-based observation studies also report that most forest fires in the country occur during this season⁵². The SSR in regions like the foothills of western Himalaya in HIM, western CEN, and northern parts of DEC and WG zones are higher than the 90th percentile severity thresholds (“Methods”) in

this season. It is interesting to note that western CEN and DEC regions have high fire weather severity even in the monsoon season JJA. This is because most of the high SSR occurs in the month of June before the southwesterly monsoon can reach these inland regions. The fire weather severity abates considerably in July–August with the advent of the monsoon precipitation. The post-monsoon season SON has the lowest SSR. In the DJF winter

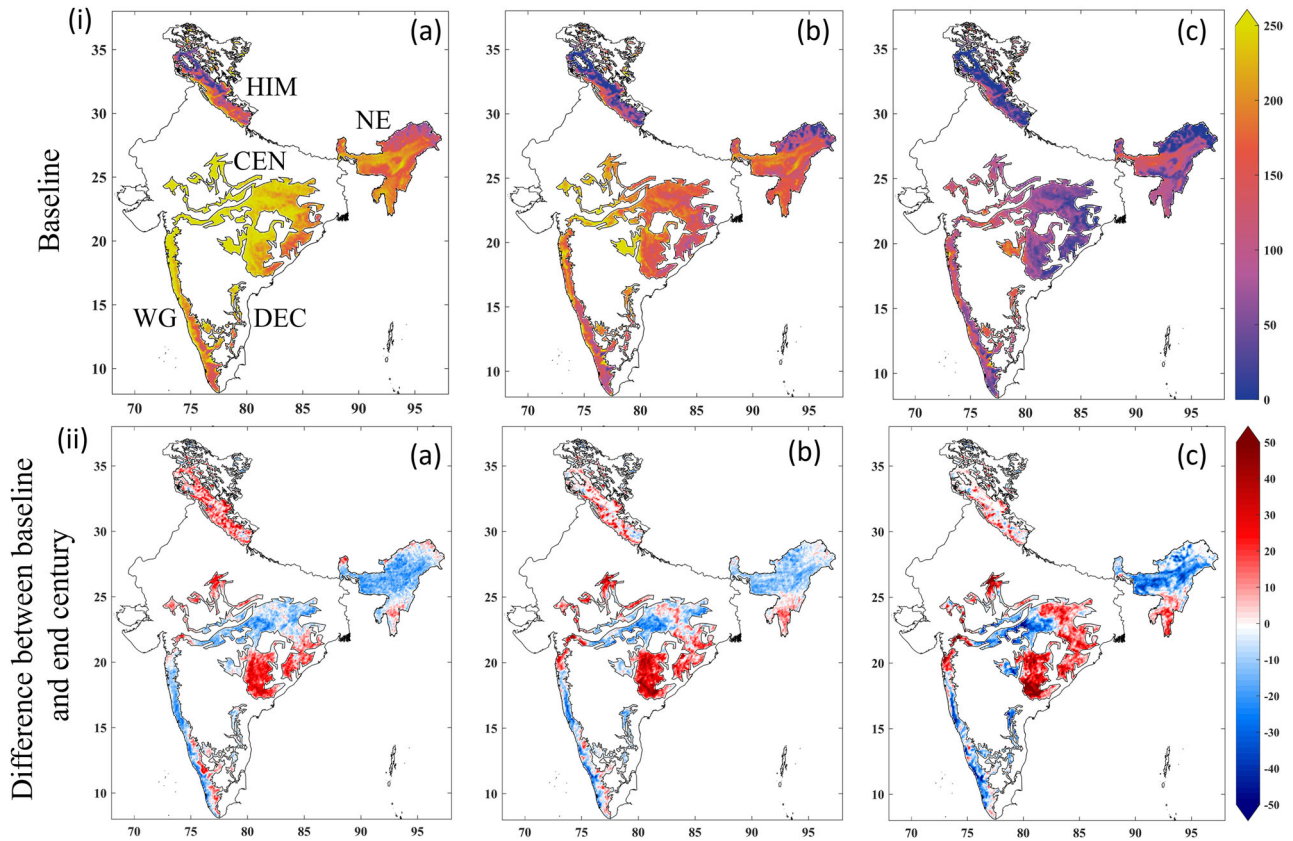


Fig. 5 Future changes in the number of days with severe fire weather. Number of days per year exceeding **a** Medium, **b** High, and **c** Very High thresholds of FWI for **(i)** the baseline period and **(ii)** change in these numbers of days expected by end-century.

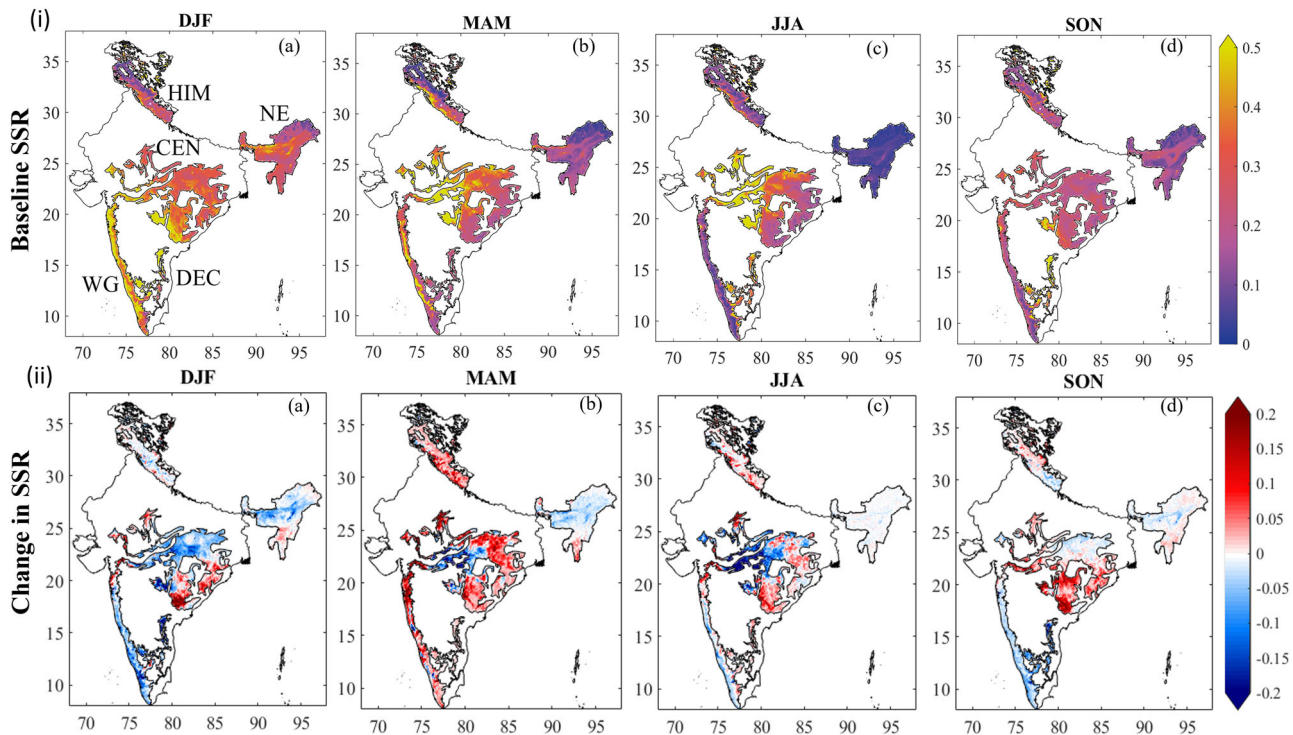


Fig. 6 Future changes in seasonal severity rating (SSR). Spatial Seasonal Severity Rating (SSR) of the **(i)** baseline and **(ii)** the difference between the end-century and baseline SSR for **a** DJF, **b** MAM, **c** JJA, and **d** SON seasons.

season, SSR is high in the WG, DEC, and southwestern CEN forest zones of southern India.

The pattern of changes in SSR in the end-century is mixed. Eastern CEN shows a consistent increase in all seasons but with varying intensity (Fig. 6-ii). WG zone shows an increasing signal only in the MAM season and a decreasing signal in other seasons. Some parts in the western CEN show a decrease in the SSR in MAM, JJA, and DJF seasons which is consistent with the reduction in the number of High and Very High fire weather days (Fig. 5-ii).

The most severe fire weather season of MAM is projected to intensify the most by the end-century (Fig. 6-ii). Relative to the baseline, the forest area, where SSR exceeds the 90th percentile threshold, is likely to increase by about 34.5%. In western CEN, a 3–5 °C warming will cause the SSR to increase by about 30%. The HIM zone is projected to become hotter by >5 °C and drier by about 8%. The SSR in this zone will also increase as a combined effect of future changes in temperature and relative humidity. In WG, SSR is projected to increase because of the ~3 °C projected warming. In contrast to this, even as MAM is projected to become ~3 °C hotter by end-century in NE, about a 15% increase in RH and pre-monsoon precipitation will decrease the future SSR.

We observe some interesting patterns in other seasons as well. In the JJA monsoon season, we see about a 50% increase in future SSR in HIM and eastern CEN regions and a 30% increase in DEC (Fig. 6-ii). This is majorly because the increase in future temperature will be greater in these regions as compared to other regions. Some monsoon deficit points in CEN are likely to experience an increase in SSR by the end-century. The high SSR regions of western CEN will experience a decrease in the future. In the post-monsoon season of SON, southern parts of CEN show a high increase in SSR (Fig. 6-iii). This is because the southern part is projected to be drier as well as hotter than the northern CEN. SSR would moderately increase by about 20–30% in some parts of HIM and NE and decrease moderately in the rest of the regions.

Although in DJF, SSR is projected to mostly decrease by 20–50% across the zones, forested areas exceeding the 90th percentile threshold would still increase by 26.5% in the end-century. The decrease in SSR is prominent in western CEN, northern WG, and NE zones. These regions are also projected to become wetter by 5–10%. SSR is projected to increase in eastern CEN, the northernmost tip of WG, and some parts of northern NE. These are the regions where projected future temperatures are higher than other regions. Overall, the decrease in SSR in all the seasons is governed by precipitation and relative humidity and the increase is governed by temperature. This finding is similar to the annual change signal in FWI discussed in the previous section (Fig. 4-i).

Fire weather danger season. We used the daily climatology of FWI to identify a fire weather danger season. We define this as a continuous period in which the daily climatology signal of FWI crosses the Medium threshold. It is important to note that the fire weather danger season is different from the fire season. Fire season is the period wherein fire occurrences are high while the fire weather danger season is the period where the fire occurrence probability is high in the presence of ignition factors.

Figure 7 depicts the daily climatology signal of FWI for both baseline and end-century periods with the shaded region depicting the uncertainty in this estimation at a $p < 0.05$ level. Results show that there is a strong periodicity in FWI in all forest zones. In general, the FWI peak is in the pre-monsoon season due to high temperatures and low humidity. This is also corroborated by SSR maps (Fig. 6-i) and observational studies⁵⁶. The FWI dips

in the post-monsoon season because of an increase in humidity. Despite the similarity in patterns, there is considerable variability in the timings of the peaks and troughs in FWI making it very challenging to define a uniform fire weather danger season across all forests of the country. If the Medium FWI threshold is considered as the fire weather danger season, then the start of the season is around December–February and the end of the season is June–September, depending on the forest type. In the HIM forests, the dry atmosphere in the pre-monsoon and winter seasons causes two distinct periods of consistently high FWI (Fig. 7a). In the DEC thorn forests the FWI peaks from the monsoon season and begins to sharply decrease by late February (Fig. 7d).

The fire weather danger season is likely to change in the future. As is evident from Fig. 7, the FWI values in the end-century period are higher during the pre-monsoon months than the baseline and lower in the winter months. This pattern is consistent with the increase in SSR in MAM discussed earlier. Figure 5 shows that in some regions, there is likely to be an increase in Medium, High, and Very High FWI days in the future that may lead to an increase in the fire weather danger season. To quantify this change, we identified the start and end days of the fire weather danger season from the FWI climatology (“Methods”, Table 1). The results show that the length of the fire weather danger season will increase up to 61 days. The highest increase is in the CEN forest zone followed by the HIM and NE zones. We also identified the nature of this change in fire weather danger season. For example, the increase in the extent of this season is mainly due to the early start of the season in the CEN, HIM, and DEC zones. In NE, the season would end later by about 15 days in April. In WG the season will slightly shift by 5 days, keeping the length of the season almost the same as the baseline.

Conclusions and discussions

We used the CFFDRS with the DSCESM high-resolution climate projections to estimate the FWI over Indian forest zones for baseline and end-century periods. We used high-quality data including the DSCESM projections and high-resolution land cover maps along with state-of-the-art tools like the WRF mesoscale model and the CFFDRS to estimate FWI. The estimates were evaluated against MODIS observations to ensure that our results are robust. We developed fire weather danger classes using an ensemble method that reduces the uncertainty in the threshold estimates. We compared the distribution of daily FWI, spatiotemporal patterns of fire weather severity, and fire weather season for the baseline and future scenarios to study the effect of climate change on fire danger. The main conclusions of the study are as follows:

- There is considerable heterogeneity in fire weather danger across the different forests of India. Forest fires can occur at considerably lower FWI values in NE forests than in the CEN, DEC, HIM, and WG forests. The FWI severity threshold is also lower in the NE zone.
- Climate change will have a strong effect on fire weather in Indian forests. The overall change in mean FWI will be about 5%. However, this change will result in the days exceeding Medium, High, and Very High severity thresholds to change by up to 60%.
- The impacts will vary between and even within forest zones. In arid and intermediate regions, temperature change will play a key role in increasing the FWI in the future. In these regions, the days with severe FWI will increase by up to 60%. However, in humid regions, fire weather danger will decrease in the future due to the more dominant effect of increased precipitation and humidity

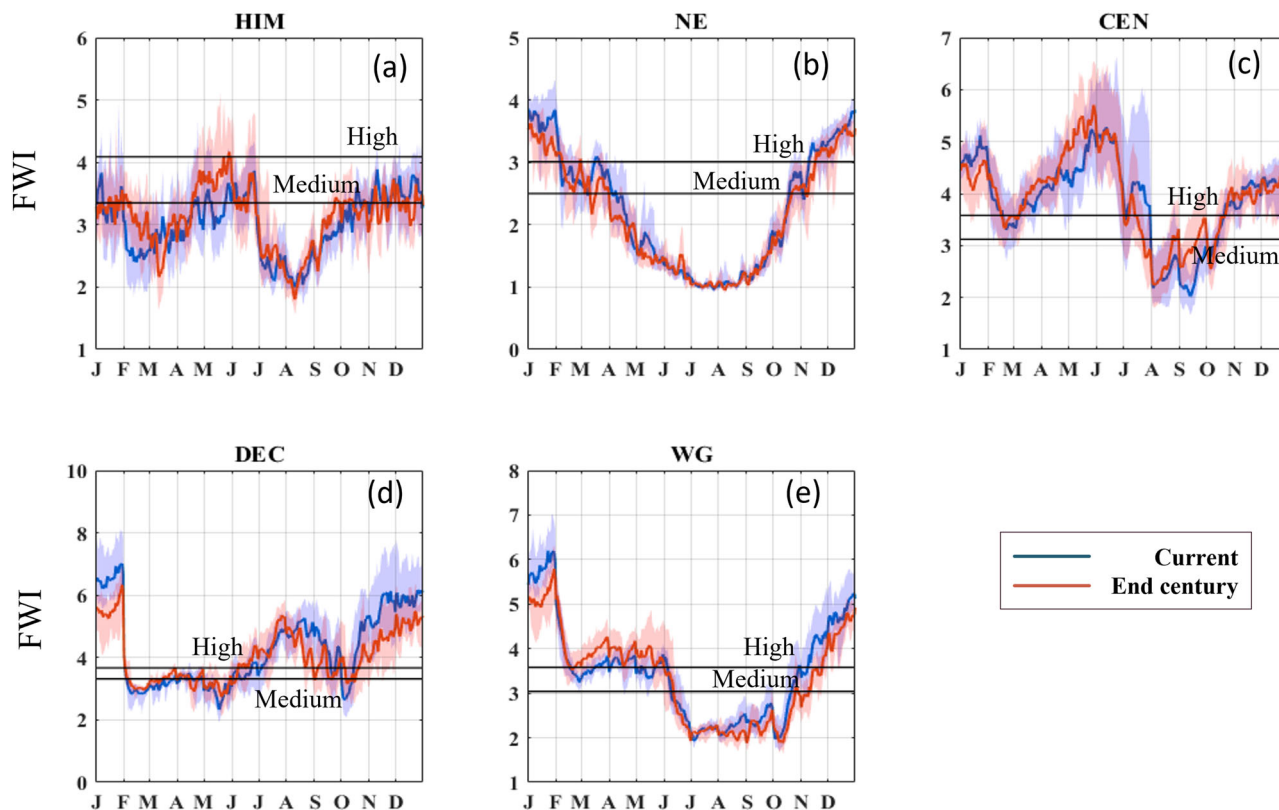


Fig. 7 Change in fire weather danger season. Fire weather danger season as derived from the daily FWI climatology for baseline (blue) and end-century (red) for **a** HIM, **b** NE, **c** CEN, **d** DEC, and **e** WG. The shaded region denotes the bootstrap uncertainty computed at 95% significance.

Table 1 Zone-wise severe fire weather danger season for baseline and end-century.

Zones	Baseline severe season	Future severe season	Diff. in days	Remarks
HIM	15th April–25th June 15th October–28th January	15th April–24th June 20th September–10th February	33	Early start and extended end
NE	15th October–1st April	15th October–15th April	15	Extension of end
CEN	10th October–1st August	20th August–20th July	61	Early start
DEC	20th June–2nd February	8th June–2nd February	12	Early start
WG	15th October–8th June	20th October–10th June	3	Shift

despite any warming. Here, the days with severe FWI will decrease by up to 40%.

- In some regions, changes in extreme rainfall events will affect fire danger where the future mean FWI change signal can be the opposite of the days with severe FWI signal.
- The pre-monsoon MAM season experiences the maximum fire weather danger. By the end-century, the seasonal severity will increase in the HIM, eastern CEN, and DEC regions covering about 55% of India’s forests during this season.
- Severe fire weather season is expected to become longer across all FWI zones with a maximum increase of about 2 months in the CEN zone.

Our study is an important advancement of the state of science. Foremost, our findings highlight that the fire weather in India is governed by the interplay between different meteorological drivers including temperature, precipitation, and humidity. We find that if precipitation and/or relative humidity increases in humid forests due to climate change, they are likely to experience a reduction in fire weather danger, despite rising temperatures. Second, our study also advances the state-of-practice by using a

very high spatial resolution that is about an order of magnitude higher than typical global-scale studies^{9,23,25,50,63}. This provides us with three distinct advantages. First, it allows us to simulate the fire weather with a high degree of granularity which is essential for the fragmented forests of India¹⁷. Second, we are able to represent the mesoscale variability in spatial patterns of precipitation that is absent in typical ESMs^{7,64}. Third, we could get a more robust estimate of forest fire events by eliminating the non-forest fires from crop residue burning by using a high-resolution forest mask. Because of this methodological improvement, we consider this work to be a useful contribution to understanding the fire-climate relationship in tropical fragmented forest systems similar to that of India.

It is important to note that fire weather is just one aspect of fire risk. Forest fire risk depends on other factors such as natural and anthropogenic ignitions, fire vulnerability of the forest type, etc. A comprehensive analysis of forest fire risk and how it will change in the future will require information on ignition and vulnerability. This information must be integrated into modeling systems to accurately predict future forest fire risk. However, fire weather is the main driver of forest fires in India. Even in the NE where anthropogenic ignition plays an important role, fire

weather is the dominant forcing that governs fire occurrence. That is why FWI is an appropriate metric that can be used to study fire risk. Indeed, various global fire management agencies rely on fire danger estimates based on weather to develop mitigation actions. Also, our future projections are just one realization of the future. For a more comprehensive assessment, multiple models and projections could be considered. However, that will be a long-term and computationally expensive endeavor.

This study has broad implications for theoretical and practical applications. This is the first attempt to explore fire weather and how it will be affected by climate change in different forest zones of India. India is a known biodiversity hotspot, and this biodiversity is affected by forest fires that play a critical role in ecosystem dynamics. Understanding the changing patterns of forest fires will advance our understanding of the effects of climate change on biodiversity and ecology. Our study also has notable ramifications for forestry practitioners. First, it identifies fire danger hotspots that need priority attention for mitigation. Second, this study clearly demonstrates that there is considerable heterogeneity in the fire danger between and even within forest zones. Hence, a national uniform threshold for fire danger is not advisable. Fire management and mitigation policies must be based on local-regional level metrics. Third, the system and the modeling framework developed in this study can be used for site-scale analysis in hotspots like national parks and other protected areas. Finally, this CFFDRS-FWI framework can also be used for fire danger forecasting provided appropriate meteorological forecasts are available.

Methods

Data. For forcing the CFFDRS-FWI for the baseline and end-century, we used high-resolution (10 km) gridded Downscaled CESM (DSCESM) data. This dataset was developed by dynamically downscaling the bias-corrected Community Earth System Model (CESMv1) climate projection under emission scenario RCP8.5 using the Weather Research and Forecasting (WRF) model over India^{65,66}. We extensively analyzed the performance of CESMv1 for the baseline period and found that it works well in India. We observed a consistent bias in the DSCESM wind speed when compared with reanalyses and ground observations. Thus, we adopted a linear scaling approach⁶⁶ to correct this bias with respect to Global Summary of the Day (GSOD) observations. The details of the bias correction are in Appendix 1 of the Supplementary Information. GSOD contains daily 24-h averages calculated from hourly station observations collected from over 9000 locations around the world. Within our forest zones, 35 GSOD stations have complete daily averages of wind speed from 2006 to 2015. We extracted the daily values from DSCESM wind speed for the grid corresponding to the GSOD station location and computed the linear and variance scaling factors. These factors were added to every grid of baseline and end-century DSCESM wind speed to correct the bias. We found the performance of the linear scaling method to be better than the variance scaling using quantile-quantile mapping against reanalysis wind data (Supplementary Fig. 1). This improved the quality of daily wind speed data (Supplementary Figs. S2 and S3). We also checked the other variables against GSOD observations and found the biases to be within acceptable ranges.

We used the Moderate Resolution Imaging Spectroradiometer (MODIS) daily active fire data to identify forest fires and evaluate the relationship between FWI and fire occurrence. The MODIS instrument aboard the Aqua and Terra satellites detects thermal anomalies and provides global information regarding the spatial distribution of forest fires and the timing of occurrence at a resolution of $1 \times 1 \text{ km}$ ⁴². We used this dataset to evaluate the

simulated FWI and compute FWI danger thresholds specific to FWI zones. For these purposes, we filtered the MODIS fire data locations from 1st January 2006 to 31st December 2015 using the forest class pixels from a land use land cover map of India⁴⁴. We then converted this filtered forest fire data to a gridded daily fire count dataset at 10 km spatial resolution, which is the same as the DSCESM meteorological dataset and the simulated FWI dataset.

CFFDRS-FWI description. The CFFDRS computes the FWI^{33,34} which is a meteorologically based numerical index used by researchers worldwide to account for the effects of weather variables on forest fuels and fires and study fire severity patterns^{35,67}. It consists of three moisture codes, namely, the Fine Fuel Moisture Code (FFMC), the Duff Moisture Code (DMC), and the Drought Code (DC) that quantify the moisture contents at 0–1 inch, 2–4 inches, and 4–8 inches depths, respectively. Then the system computes two intermediate indices, namely, the Initial Spread Index (ISI) and the Buildup Index (BUI). The ISI combines the effect of wind speed and top layer moisture from FFMC to compute the rate of spread of fire. BUI is computed from DMC and DC representing the fuel available for combustion. FWI is calculated from ISI and BUI. We wrote a MATLAB code which is available on GitHub to compute the indices based on the equations provided in Wagner³³. The input provided to this code is derived from DSCESM. The variables are 12 noon IST values of 2 m temperature, relative humidity, bias-corrected wind speed, and 12 noon IST–12 noon IST accumulated precipitation.

System calibration and initialization. The equations of the CFFDRS-FWI system and the danger thresholds³³ were designed primarily for use in the Canadian climate. We applied the following calibration steps to implement this system in India.

Latitude adjustment. The FFMC index, which represents the fuel load of the topmost layer directly in contact with the near-surface atmosphere, depends heavily on meteorological variations⁶⁷, and hence it does not need any adjustment. However, DMC and DC need adjustment because these computations are influenced by the daylight factor that depends upon the latitude of the region and the date-of-year values³³. For our simulations, we considered the latitude value at every grid point to compute the corresponding day lengths. In potential evapotranspiration (PET) computation for DC, we make 2 assumptions: (1) The latitudes close to the equator (<20 in the northern hemisphere) receive consistent heating throughout the year⁴¹ and (2) the PET in the higher latitudes is dependent on the month of calculation.

Spin-up simulations. Computation of FWI requires initialization of FFMC, DMC, and DC values from the previous day. A 5-year long spin-up simulation was conducted for each scenario by initializing the system with default FFMC, DMC, and DC values of 85, 6, and 15, respectively, for every forested grid cell. The FFMC, DMC, and DC values for each forest grid cell at the end of the spin-up were used to initialize that grid cell for the simulations for the baseline and future scenarios. We observed that the values at the end of the spin-up varied across different forest zones and they were quite different from the default values. A similar finding has been reported by other studies^{38,41,68}. Another interesting feature was that the parameters appeared to stabilize in about 1 year (Fig. 8). The figure shows that the annual cycles in years 2–5 are similar while year 1 is quite different. This suggests that a 1-year spin-up might be sufficient in this region.

Statistical methods. To quantitatively understand the relationship between FWI and fire occurrence, we compared the daily

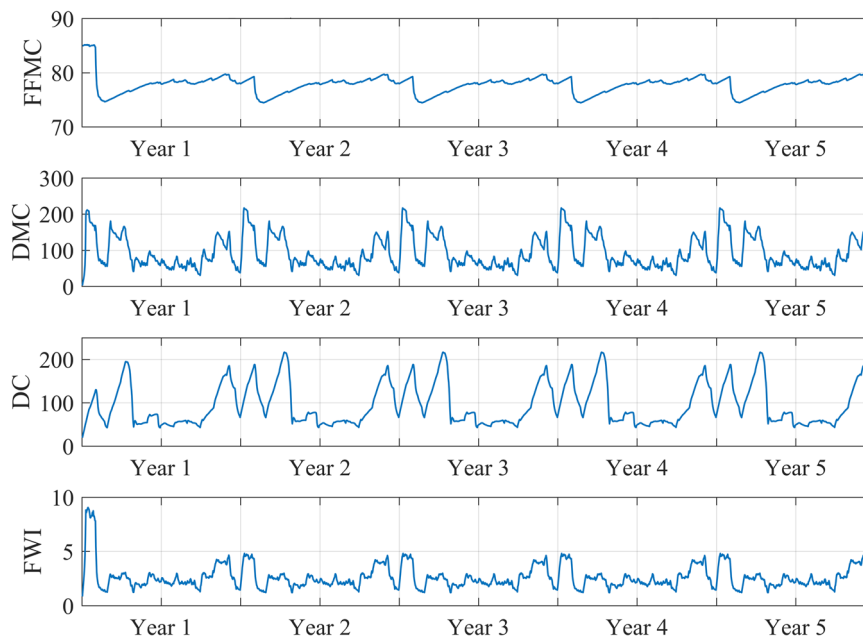


Fig. 8 Spin-up for stable values of intermediate indices. FFMC, DMC, DC and FWI values for the 5-year spin-up simulation averaged over all forest grid cells.

FWI simulated for the baseline period with MODIS active fire data. For this, we converted the MODIS data into daily fire count per 10 Km pixel data. First, we applied three non-parametric statistical tests namely The Chi-square test of association/independence⁴⁵, Yule's correlation⁴⁶ and Fisher's exact test⁴⁷. All three tests first specify if there exists any non-random relationship between the two datasets. The extent of this relationship is specified further by Yule's correlation coefficient and Fisher's odds ratio. Yule's coefficient gives a correlation parameter between 0 and 1 with higher values signifying a stronger relationship. Fisher's odds ratio is a measure of the relative odds of the occurrence of the outcome of interest which in our case is more fire count associated with higher FWI values. Second, we plotted a scatterplot of FWI percentile bins vs. the count of fire events corresponding to those percentile values. The percentile bins were computed from the daily FWI dataset at all grid cells within a particular zone. Even the fire count is aggregated daily fire count for 10 years between the percentile bins. These curves showed us how the fire counts are spread across various percentile levels of FWI. We also determined the best-fit curves to determine the nature of the curve and the coefficient of determination.

Fire danger classification. We classified the FWI values into five fire danger classes namely Low, Medium, High, Very High, and Extreme. The default approach to calculate the fire danger class thresholds is to define the lower limit for the Extreme class using the FWI dataset³³. We selected this value to be the 99th percentile of FWI in each zone. Then we used geometric progression to define the limits of other danger classes. However, using this approach, the conditional probability⁶⁹ of fires occurring beyond High and Very High classes in few zones saturated at 1. Thus, we used an ensemble of five different methods by using the fire count information in addition to the FWI dataset to characterize limiting FWI for each danger class.

1. Logistic regression approach⁷⁰ is a predictive technique involving a binary outcome. The basic equation is

$$y = 1/(1 + \exp(\beta_0 + \beta_1x)) \quad (1)$$

where y is the predictand and x is the predictor variable and β_0 and β_1 are the regression coefficients. We provided the fire data converted into a nominal variable along with the FWI value of the corresponding grid cell as inputs and fire occurrence probability was computed as a function of both. Then, we considered the FWI values corresponding to 0.2, 0.5, 0.7, and 0.9 fire probability³⁸ as the thresholds for Low, Moderate, High, and Very High danger classes respectively.

2. A percentile-based method^{71,72} classifies the Low, Moderate, High, and Very High danger classes by the 97th, 90th, 45th, and 22nd percentile values of FWI from each region, respectively.
3. A geometric progression method³³ limits the extreme fire danger days in a fire season to not more than 3%. Danger classes were based on FWI values corresponding to when the percentage of days throughout the fire seasons are 43, 26, 13, and 3% for each class respectively³⁹.
4. A system based on percentages of fires occurring beyond a particular threshold was introduced by ref. ⁷³. FWI values beyond which 40%, 65%, 87%, and 96% of all fires occurred defined the danger class thresholds respectively.
5. K-means clustering⁷⁴ is a machine learning-based clustering technique. Based on MODIS fire occurrence data converted to values of 1 for presence and 0 for absence (absence data was randomly sampled) and their corresponding FWI values, we applied K-means clustering (10 years—all grid points) and separated the FWI dataset into 5 danger class clusters. It took 10^6 iterations to get the results to converge.

We averaged the highest value in each threshold class computed from the above five methods. These characterized the limiting values of each fire danger class. We also evaluated the conditional probability distribution⁶⁹ of this ensemble approach.

Future FWI projections. We computed all the components of the FWI system using the DSCESM meteorological input for the baseline (2006–2015) and the end-century (2091–2100) period. Then, we created the final output FWI dataset at a daily temporal resolution and spatial resolution of 10×10 km for both periods.

First, we computed the climatological change in FWI by subtracting the baseline 10-year average from the end-century 10-year average of FWI. Then, to understand the major contributor variable causing the climatological change in FWI, we performed 4 sensitivity experiments. In each sensitivity experiment, we simulated end-century FWI by using end-century values of one variable and retaining the baseline values of other variables. This separated the individual impacts of expected future change in each variable over the future change in FWI. For each spatial pixel, we identified the variable whose sensitivity was maximum with respect to baseline FWI and considered that variable as the major contributor to future FWI change. We also used a modified scale based on De Martonne's aridity index^{54,55} to classify the pixels into arid, intermediate, and humid. We classified the pixels with index values less than 20 as arid, 20–35 as intermediate and greater than 35 as humid. We then analyzed the contributor variables against this modified aridity index.

Then, we computed a non-parametric probability density estimation of daily FWI within a particular FWI zone using Epanechnikov Kernel density estimation (KDE) with an optimally computed bandwidth for the baseline and end-century periods^{75,76}. From this, we calculated the shift in average daily FWI for each zone using the Bootstrap confidence interval for the mean parameter at a $p < 0.05$. This method of bootstrapping the confidence interval is majorly used to optimize the length of the confidence interval and adopts a less conservative approach as compared to the asymptotic method^{77–79}. Thus, this method was most suitable for our application as it ensured that the changes in fire weather danger by the end-century were not undermined. We also computed the number of days exceeding a certain threshold like Medium, High, and Very High fire dangers for both periods. We then plotted the baseline values spatially as a reference along with the difference between the end-century and baseline severe fire weather days.

Daily Severity Rating (DSR), an additional component of the FWI system, is a numeric measure of the difficulty of controlling fires³³. Based on the FWI, it represents the expected effort required for fire suppression. Other studies⁸⁰ have established the relationship between DSR and fire occurrences.

$$DSR = 0.0272 * FWI^{1.77} \quad (2)$$

Higher FWI values are emphasized through the power relation. The DSR can be accumulated over time as the cumulative DSR, or it may be averaged over time as the Seasonal Severity Rating (SSR) as in Eq. 3

$$SSR = \sum_{i=1}^n DSR_i / n \quad (3)$$

where DSR_i is the DSR value for day i , and n is the total number of days. We computed SSR for the baseline and future periods to analyze the seasonal changes in fire danger. These parameters were also filtered with the forest layer shapefiles and divided into zones. We considered a value of 90th percentile SSR in the baseline scenario as a threshold beyond which the fire potential becomes severe. These SSR thresholds for HIM, NE, CEN, DEC, and WG zones are 0.52, 0.3, 0.59, 0.8, and 0.62 respectively.

We defined a 'fire weather danger season' as a period in which the fire occurrence probability is high. We considered the part of the daily climatology curve beyond the Medium fire danger threshold of FWI as this fire weather danger season.

Data availability

The DSCESM meteorological dataset⁶⁵ is archived with the World Data Centre for Climate which can be accessed from https://doi.org/10.26050/WDC/WRFI0km_wbc_C5_forc_oIndia. The National Centers for Environmental Information (NCEI) provides

the GSOD dataset at various stations which can be accessed from <https://www.ncei.noaa.gov/access/search/data-search/global-summary-of-the-day>. The MODIS active fire data is distributed by Fire Information for Resource Management System (FIRMS) and archived data from 2003 to the present can be accessed from https://firms.modaps.eosdis.nasa.gov/active_fire/. The computed FWI daily dataset for both the baseline and end-century time slices are publicly available in a Zenodo archive and can be accessed from <https://doi.org/10.5281/zenodo.10126266>.

Code availability

The modifiable MATLAB code to compute FWI is available on the GitHub repository (https://github.com/anasuya993/CFFDRS-FWI_India/blob/main/CFFDRS_FWI_year_ABIitd.m, last access: 28 August 2023) and the frozen version 1 is available in a Zenodo archive (<https://doi.org/10.5281/zenodo.10047237>).

Received: 23 February 2023; Accepted: 15 November 2023;

Published online: 02 December 2023

References

- Flannigan, M. D., Amiro, B. D., Logan, K. A., Stocks, B. J. & Wotton, B. M. Forest fires and climate change in the 21st century. *Mitig. Adapt. Strateg. Glob. Chang.* **11**, 847–859 (2006).
- Gonzalez, P., Neilson, R. P., Lenihan, J. M. & Drapek, R. J. Global patterns in the vulnerability of ecosystems to vegetation shifts due to climate change. *Glob. Ecol. Biogeogr.* **19**, 755–768 (2010).
- Abatzoglou, J. T. & Williams, A. P. Impact of anthropogenic climate change on wildfire across western US forests. *Proc. Natl Acad. Sci. USA* **113**, 11770–11775 (2016).
- Abram, N. et al. Connections of climate change and variability to large and extreme forest fires in southeast Australia. *Commun. Earth Environ.* **2**, 8 (2021).
- Canadell, J. et al. Multi-decadal increase of forest burned area in Australia is linked to climate change. *Nat. Commun.* **12**, 6921 (2021).
- Caretta, M. A. et al. *Water. Climate Change 2022: Impacts, Adaptation and Vulnerability*. Contribution of Working Group II to the Sixth Assessment Report of the Intergovernmental Panel on Climate Change, Vol. 15 (IPCC, 2016).
- Liu, Y., Stanturf, J. & Goodrick, S. Trends in global wildfire potential in a changing climate. *For. Ecol. Manag.* **259**, 685–697 (2010).
- Wotton, B. Forest fire occurrence and climate change in Canada. *CSIRO Publishing* **19**, 253–271 (2010).
- Moritz, M. A. et al. Climate change and disruptions to global fire activity. *Ecosphere* **3**, art49 (2012).
- Liu, Y., Goodrick, S. L. & Stanturf, J. A. Future US wildfire potential trends projected using a dynamically downscaled climate change scenario. *For. Ecol. Manag.* **294**, 120–135 (2013).
- Krikken, F., Lehner, F., Hausteiner, K., Drobyshev, I. & Jan Van Oldenborgh, G. Attribution of the role of climate change in the forest fires in Sweden 2018. *Nat. Hazards Earth Syst. Sci.* **21**, 2169–2179 (2021).
- Wotton, B. M. & Flannigan, M. D. Length of the fire season in a changing climate. *For. Chron.* **69**, 187–192 (1993).
- Flannigan, M. D., Stocks, B. J. & Wotton, B. M. Climate change and forest fires. *Sci. Total Environ.* **262**, 221–229 (2000).
- Masson-Delmotte, V. & Zhou, B. *Climate Change—The Physical Science Basis* (IPCC, 2021).
- Seneviratne, S. I. et al. Weather and climate extreme events in a changing climate. *Climate Change 2021—The Physical Science Basis*, 1513–1766 (Cambridge University Press, 2023).
- India State Forest Report 2021, Forest Survey of India* (2022).
- Reddy, C. S., Sreelekshmi, S., Jha, C. S. & Dadhwal, V. K. National assessment of forest fragmentation in India: Landscape indices as measures of the effects of fragmentation and forest cover change. *Ecol. Eng.* **60**, 453–464 (2013).
- Chaturvedi, R. K., Joshi, J., Jayaraman, M., Bala, G. & Ravindranath, N. H. Multi-model climate change projections for India under representative concentration pathways. *Curr. Sci.* **103**, 791–802 (2012).
- Krishnan, R. et al. *Assessment of Climate Change over the Indian Region: A Report of the Ministry of Earth Sciences (MoES), Government of India*, 226 (Springer, 2020).
- Littell, J. S., Peterson, D. L., Riley, K. L., Liu, Y. & Luce, C. H. A review of the relationships between drought and forest fire in the United States. *Glob. Chang. Biol.* **22**, 2353–2369 (2016).
- Fanin, T. & van der Werf, G. Precipitation–fire linkages in Indonesia (1997–2015). *Biogeosciences* **14**, 3995–4008 (2017).

22. Pechony, O. & Shindell, D. T. Driving forces of global wildfires over the past millennium and the forthcoming century. *Proc. Natl Acad. Sci. USA* **107**, 19167–19170 (2010).
23. Sun, Q. et al. Global heat stress on health, wildfires, and agricultural crops under different levels of climate warming. *Environ. Int.* **128**, 125–136 (2019).
24. Scholze, M., Knorr, W., Arnell, N. W. & Prentice, I. C. A climate-change risk analysis for world ecosystems. *Proc. Natl Acad. Sci. USA* **103**, 13116–13120 (2006).
25. Quilcaille, Y., Batibeniz, F., Ribeiro, A. F. S., Padrón, R. S. & Seneviratne, S.I. Fire weather index data under historical and shared socioeconomic pathway projections in the 6th phase of the Coupled Model Intercomparison Project from 1850 to 2100. *Earth Syst. Sci. Data* **15**, 2153–2177 (2023).
26. Schroeder, M. J. & Buck, C. C. *Forest Weather: A Guide for Application of Meteorological Information to Forest Fire Control Operations* (No. 360) (US Department of Agriculture, 1970).
27. Flannigan, M. D., Logan, K. A., Amiro, B. D., Skinner, W. R. & Stocks, B. J. Future area burned in Canada. *Clim. Change* **72**, 1–16 (2005).
28. Kirchmeier-Young, M. C., Gillett, N. P., Zwiers, F. W., Cannon, A. J. & Anslow, F. S. Attribution of the influence of human-induced climate change on an extreme fire season. *Earths Future* **7**, 2–10 (2019).
29. Barbero, R., Abatzoglou, J. T., Larkin, N. K., Kolden, C. A. & Stocks, B. Climate change presents increased potential for very large fires in the contiguous United States. *Int. J. Wildland Fire* **24**, 892–899 (2015).
30. Dimitrakopoulos, A. P. & Papaioannou, K. K. Flammability assessment of Mediterranean forest fuels. *Fire Technol.* **37**, 143–152 (2001).
31. Vadrevu, K. P. et al. Trends in vegetation fires in south and southeast Asian countries. *Sci. Rep.* **9**, 1–13 (2019).
32. Abatzoglou, J. T., Williams, A. P. & Barbero, R. Global emergence of anthropogenic climate change in fire weather indices. *Geophys. Res. Lett.* **46**, 326–336 (2019).
33. Van Wagner, C. E. *Development and Structure of the Canadian Forest Fire Weather Index System*. Forestry Technical Report (Canadian Forestry Service, 1987).
34. Stocks, B. J. et al. The Canadian forest fire danger rating system: an overview. *For. Chron.* **65**, 450–457 (1989).
35. Wotton, B. M. Interpreting and using outputs from the Canadian Forest Fire Danger Rating System in research applications. *Environ. Ecol. Stat.* **16**, 107–131 (2009).
36. Viegas, D. X., Bovio, G., Ferreira, A., Nosenzo, A. & Sol, B. Comparative study of various methods of fire danger evaluation in southern Europe. *Int. J. Wildland Fire* **9**, 235–246 (1999).
37. Groot, W. J. D., Field, R. D., Brady, M. A., Roswintarti, O. & Mohamad, M. Development of the Indonesian and Malaysian fire danger rating systems. *Mitig. Adapt. Strateg. Chang.* **12**, 165–180 (2007).
38. Dimitrakopoulos, A. P., Bemmerzouk, A. M. & Mitsopoulos, I. D. Evaluation of the Canadian fire weather index system in an eastern Mediterranean environment. *Meteorol. Appl.* **18**, 83–93 (2011).
39. Tian, X. et al. Wildfires and the Canadian Forest Fire Weather Index system for the Daxing'anling region of China. *Int. J. Wildland Fire* **20**, 963–973 (2011).
40. Karali, A. et al. Sensitivity and evaluation of current fire risk and future projections due to climate change: the case study of Greece. *Nat. Hazards Earth Syst. Sci.* **14**, 143–153 (2014).
41. de Groot, W. J. & O'Loughlin, K. Developing a global early warning system for wildland fire. *For. Ecol. Manag.* **234**, 1 (2006).
42. Giglio, L., Desloires, J., Justice, C. O. & Kaufman, Y. J. An enhanced contextual fire detection algorithm for MODIS. *Remote Sens. Environ.* **87**, 273–282 (2003).
43. Peel, M. C., Finlayson, B. L. & McMahon, T. A. Updated world map of the Köppen-Geiger climate classification. *Hydrol. Earth Syst. Sci.* **11**, 1633–1644 (2007).
44. Roy, P. S. et al. New vegetation type map of India prepared using satellite remote sensing: comparison with global vegetation maps and utilities. *Int. J. Appl. Earth Obs. Geoinf.* **39**, 142–159 (2015).
45. McHugh, M. L. The chi-square test of independence. *Biochem. Med.* **23**, 143–149 (2013).
46. Yule, G. U. On the theory of correlation. *J. R. Stat. Soc.* **60**, 812–854 (1897).
47. Upton, G. J. Fisher's exact test. *J. R. Stat. Soc. A Stat. Soc.* **155**, 395–402 (1992).
48. Badarinath, K. V. S., Kharol, S. K. & Chand, T. K. Use of satellite data to study the impact of forest fires over the northeast region of India. *IEEE Geosci. Remote Sens. Lett.* **4**, 485–489 (2007).
49. Puri, K., Areendran, G., Raj, K., Mazumdar, S. & Joshi, P. K. Forest fire risk assessment in parts of northeast India using geospatial tools. *J. For. Res.* **22**, 641–647 (2011).
50. Bedia, J. et al. Global patterns in the sensitivity of burned area to fire-weather: implications for climate change. *Agric. For. Meteorol.* **214–215**, 369–379 (2015).
51. Joseph, S., Anitha, K. & Murthy, M. S. R. Forest fire in India: a review of the knowledge base. *J. For. Res.* **14**, 127–134 (2009).
52. Forest Survey of India. *State of Forest Report (ISFR)*. <https://www.fsi.nic.in/forest-report-2021> (2021).
53. Reddy, C. S., Krishna, P. H., Anitha, K. & Joseph, S. Mapping and inventory of forest fires in Andhra Pradesh, India: current status and conservation needs. *Int. Sch. Res. Notices* **2012**, 380412 (2012).
54. De Martonne, E. Aridité et indices d'aridité. *C. R. Acad. Sci.* **181**, 1395–1398 (1926).
55. Ullah, S. et al. Spatiotemporal changes in global aridity in terms of multiple aridity indices: an assessment based on the CRU data. *Atmos. Res.* **268**, 105998 (2022).
56. Fulé, P. Z., Garkoti, S. C. & Semwal, R. L. Frequent burning in chir pine forests, Uttarakhand, India. *Fire Ecol.* **17**, 1–11 (2021).
57. Vadrevu, K. P., Giglio, L. & Justice, C. Satellite based analysis of fire-carbon monoxide relationships from forest and agricultural residue burning (2003–2011). *Atmos. Environ.* **64**, 179–191 (2013).
58. Verma, S., Singh, D., Mani, S. & Jayakumar, S. Effect of forest fire on tree diversity and regeneration potential in a tropical dry deciduous forest of Mudumalai Tiger Reserve, Western Ghats, India. *Ecol. Process* **6**, 1–8 (2017).
59. Srivastava, P. & Garg, A. Forest fires in India: regional and temporal analyses. *J. Tropical For. Sci.* **25**, 228–239 (2013).
60. Herawati, H. & Santoso, H. Tropical forest susceptibility to and risk of fire under changing climate: a review of fire nature, policy and institutions in Indonesia. *For. Policy Econ.* **13**, 227–233 (2011).
61. Halofsky, J. E., Peterson, D. L. & Harvey, B. J. Changing wildfire, changing forests: the effects of climate change on fire regimes and vegetation in the Pacific Northwest, USA. *Fire Ecol.* **16**, 1–26 (2020).
62. Augustin, F. et al. Projected changes in fire activity and severity feedback in the spruce-feather moss forest of western Quebec, Canada. *Trees For. People* **8**, 9 (2022).
63. Son, R. et al. Changes in fire weather climatology under 1.5 °C and 2.0 °C warming. *Environ. Res. Lett.* **16**, 034058 (2021).
64. Maraun, D. et al. Precipitation downscaling under climate change: recent developments to bridge the gap between dynamical models and the end user. *Rev. Geophys.* **48**, RG3003 (2010).
65. Barik, A., Sahoo, S. K., Kumari, S. & Baidya Roy, S. *10 km Gridded Hydrometeorological Dataset Developed by Dynamical Downscaling of the Bias-corrected Cnrip5 Cesm Rcp8.5 Projections over India for Current (2006–2015) and Future (2091–2100) Periods Using WRF*. World Data Center for Climate (WDCC) at DKRZ https://www.wdc-climate.de/ui/entry?acronym=WRF10km_wbc_C5_forc_oIndia (2021).
66. Li, D. et al. Statistical bias correction for simulated wind speeds over CORDEX-East Asia. *Earth Space Sci.* **6**, 200–211 (2019).
67. Vitolo, C., Di Giuseppe, F., Krzeminski, B. & San-Miguel-Ayanz, J. A 1980–2018 global fire danger re-analysis dataset for the Canadian Fire Weather Indices. *Sci. Data* **6**, 190032 (2019).
68. Dowdy, A. J., Mills, G. A., Finkele, K. & De Groot, W. *Australian Fire Weather as Represented by the McArthur Forest Fire Danger Index and the Canadian Forest Fire Weather Index*, 91 (Centre for Australian Weather and Climate Research, 2009).
69. Hall, P., Racine, J. & Li, Q. Cross-validation and the estimation of conditional probability densities. *J. Am. Stat. Assoc.* **99**, 1015–1026 (2004).
70. Cramer, J. S. *The Origins of Logistic Regression* (Tinbergen Institute, 2002).
71. Andrews, P. L. & Bradshaw, L. S. *FIRE: Fire Information Retrieval and Evaluation System—A Program for Fire Danger Rating Analysis*. Gen. Tech. Rep. (US Department of Agriculture, 1997).
72. Rainha, M., Fernandes, P. M. & Viegas, D. X. Using the Canadian Fire Weather Index (FWI) in the Natural Park of Montesinho, NE Portugal: calibration and application to fire management. In *Proc. IV International Conference on Forest Fire Research* (2002).
73. Varela, V. et al. Projection of forest fire danger due to climate change in the French Mediterranean region. *Sustainability* **11**, 4284 (2019).
74. Morissette, L. & Chartier, S. The k-means clustering technique: general considerations and implementation in *Mathematica*. *Tutor. Quant. Methods Psychol.* **9**, 15–24 (2013).
75. Epanechnikov, V. Nonparametric estimation of a multidimensional probability density. *Teoriya Veroyatnostei i ee Primeneniya* **14**, 156–161 (1969).
76. Samiuddin, M. & El-Sayyad, G. M. On nonparametric kernel density estimates. *Biometrika* **77**, 865–874 (1990).
77. DiCiccio, T. J. & Efron, B. Bootstrap confidence intervals. *Stat. Sci.* **11**, 189–228 (1996).
78. Kundu, D. & Ganguly, A. *Analysis of Step-Stress Models: Existing Results and Some Recent Developments* (Academic Press, 2017).
79. Ramachandran, K. M. & Tsokos, C. P. *Mathematical Statistics with Applications in R* 2nd edn (Academic Press, 2014).
80. Lehtonen, I., Venäläinen, A., Kämäläinen, M., Peltola, H. & Gregow, H. Risk of large-scale fires in boreal forests of Finland under changing climate. *Nat. Hazards Earth Syst. Sci.* **16**, 239–253 (2016).

Author contributions

S.B.R. conceptualized the work. A.B. designed the methodology and performed the analyses under the close supervision of S.B.R. A.B. and S.B.R. compiled the results and wrote the manuscript.

Competing interests

The authors declare no competing interests.

Additional information

Supplementary information The online version contains supplementary material available at <https://doi.org/10.1038/s43247-023-01112-w>.

Correspondence and requests for materials should be addressed to Anasuya Barik or Somnath Baidya Roy.

Peer review information *Communications Earth & Environment* thanks Yann Quilcaille and the other anonymous reviewer(s) for their contribution to the peer review of this work. Primary handling editors: Yongqiang Liu and Aliénor Lavergne. A peer review file is available.

Reprints and permission information is available at <http://www.nature.com/reprints>

Publisher's note Springer Nature remains neutral with regard to jurisdictional claims in published maps and institutional affiliations.



Open Access This article is licensed under a Creative Commons Attribution 4.0 International License, which permits use, sharing, adaptation, distribution and reproduction in any medium or format, as long as you give appropriate credit to the original author(s) and the source, provide a link to the Creative Commons license, and indicate if changes were made. The images or other third party material in this article are included in the article's Creative Commons license, unless indicated otherwise in a credit line to the material. If material is not included in the article's Creative Commons license and your intended use is not permitted by statutory regulation or exceeds the permitted use, you will need to obtain permission directly from the copyright holder. To view a copy of this license, visit <http://creativecommons.org/licenses/by/4.0/>.

© The Author(s) 2023